

# BRILLOUIN EFFECT CHARACTERIZATION IN ALL-RAMAN AMPLIFIED $4 \times 40$ GB/s WDM SYSTEM

M. J. Pontes,<sup>1</sup> M. E. V. Segatto,<sup>1</sup> A. P. L. Barbero,<sup>2</sup> M. T. M. Rocco Giraldi,<sup>3</sup> A. M. Rocha,<sup>4</sup> B. Neto,<sup>4</sup> J. C. W. Costa,<sup>5</sup> M. A. G. Martinez,<sup>6</sup> O. Frazao,<sup>7</sup> J. M. Baptista,<sup>7</sup> H. Salgado,<sup>7</sup> A. L. J. Teixeira,<sup>4</sup> and P. S. André<sup>4</sup>

<sup>1</sup> Department of Electrical Engineering, Federal University of Espírito Santo, Vitória, ES, Brazil

<sup>2</sup> Department of Telecommunications Engineering, UFF, Niterói, RJ, Brazil

<sup>3</sup> Department of Electrical Engineering, IME, Rio de Janeiro, RJ, Brazil; Corresponding author: mtmrocco@ime.ub.br

<sup>4</sup> Instituto de Telecomunicações, Aveiro, Portugal

<sup>5</sup> UFPA, Belém, PA, Brazil

<sup>6</sup> CEFET-RJ, Rio de Janeiro, RJ, Brazil

<sup>7</sup> INESC-Porto, Porto, Portugal

Received 25 August 2011

**ABSTRACT:** This article analyzes experimentally the limitations observed in a 45 km Raman amplified  $4 \times 40$  Gb/s transmission system operating under multiple pump and single high pump power configurations. A signal-to-noise ratio of 19.2 dB, an extinction ratio of 10.4 dB and a jitter of 1097 fs are achieved for moderate pump powers and higher order stimulated Brillouin scattering lines give rise to system degradation for pump power levels more than 0.5 W. © 2012 Wiley Periodicals, Inc. Microwave Opt Technol Lett 54:1403–1407, 2012; View this article online at [wileyonlinelibrary.com](http://wileyonlinelibrary.com). DOI 10.1002/mop.26827

**Key words:** fiber optics amplifiers; fiber optics communications; stimulated Brillouin scattering

## 1. INTRODUCTION

The permanent demand for high capacity fiber communication systems stimulated the development of multiwavelength technologies such as wavelength division multiplexing (WDM). To realize long-range and extra-capacity fiber communication, research works have been focused on fiber Raman amplifiers [1]. The performance of WDM systems considering Raman amplifiers has been analyzed over the last few years [2, 3]. This is the case of a WDM fiber-radio network using distributed Raman amplifiers (DRAs) that enhances the link optical output power [4]. The impairment caused by nonlinear effects and the

interplay between them is involved in such studies and are important issues to be addressed in the incoming WDM networks.

Broadband Raman amplifiers require the use of multiple high pump power lasers. As a consequence, the total pump power available increases in the networks and can lead to undesirable nonlinear effects such as stimulated Brillouin scattering (SBS). This effect can be intensified in single mode fiber (SMF) transmission systems using narrow-linewidth single frequency lasers [5] and give place to interchannel interference between counter-propagating signal waves in bidirectional transmission systems [6]. SBS has been already reported in a specific configuration using DRAs [7]. However, the continued Raman pump lasers evolution has enhanced the pump power and also reduced the spectral linewidth of such devices.

The observation of the Brillouin effect due to an excessive optical power inside the fiber that leads to SBS sidebands has been reported in Ref. 8. The effect of SBS was also observed in a specific configuration of Raman amplifier, as reported in Ref. 7. In this case, the impact of SBS in a double-pass discrete Raman amplified  $4 \times 10$  Gb/s system was experimentally investigated along with SBS threshold.

In this article, we analyze experimentally the limitations of a Raman amplified WDM transmission system at 40 Gb/s-per-channel. Four input channels coupled to a 40 km of SMF link with 5 km of dispersion compensating fiber (DCF) generate a 160-Gb/s WDM system. We have evaluated the impact of Raman multi-pump and Raman single high pump power configurations on the system in the generation of SBS lines. The DCF length was calculated to fully compensate the fiber dispersion and also to enhance the amplifier gain. System performance was verified through eye diagram and optical WDM spectrum measurements.

This article is organized as follows: Section 2 discusses the experimental setup and its specifications. The experimental results are presented and discussed in Section 3. The conclusions are in Section 4.

## 2. EXPERIMENTAL SETUP

The experimental setup consists of four WDM channels operating at 40 Gb/s each as shown in Figure 1. In the transmitter side, four DFB laser diodes centered, respectively, at  $\lambda_1 = 1548.54$  nm,  $\lambda_2 = 1550.12$  nm,  $\lambda_3 = 1551.60$  nm, and  $\lambda_4 = 1552.69$  nm were multiplexed (using a  $4 \times 1$  WDM coupler) and

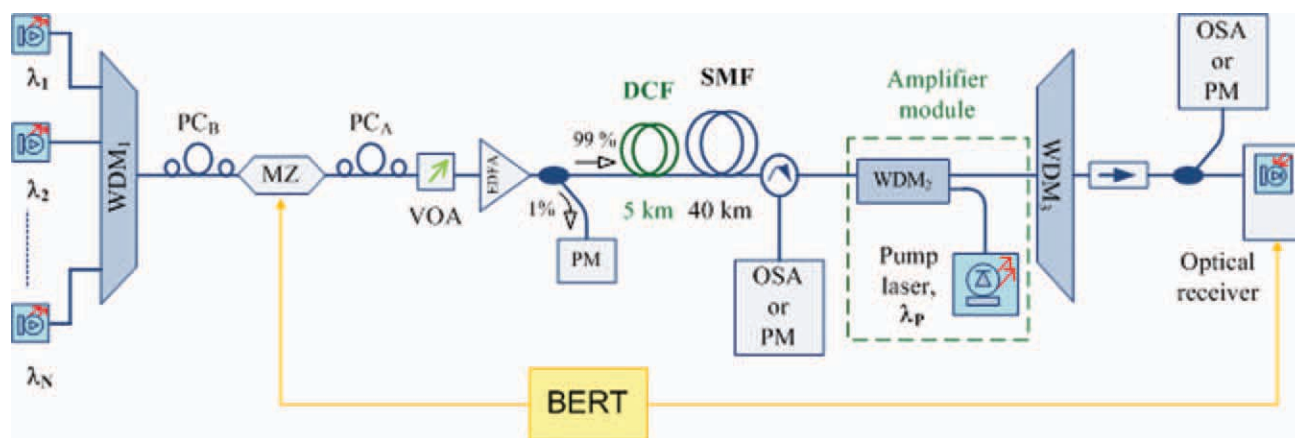


**Figure 1** WDM communication system using Raman amplifier set with DCF + SMF characterized at a transmission rate of 40 Gb/s, per channel. OSA: optical spectrum analyzer; PM: power meter; BERT: bit error rate tester; MZ: Mach-Zehnder modulator, PC: polarization controller, VOA: variable optical attenuator, EDFA: erbium doped fiber amplifier. [Color figure can be viewed in the online issue, which is available at [wileyonlinelibrary.com](http://wileyonlinelibrary.com)]

**TABLE 1** Fibers Parameters

Parameter	Fiber Type	
	SMF	DCF
Attenuation (dB/km)	0.198@ 1550 nm	1.260@ 1487 nm
Dispersion @ 1550 nm (ps/nm km)	16.5	−132.0

simultaneously modulated by a LiNbO<sub>3</sub> Mach–Zehnder modulator with a 40-Gb/s 2<sup>1</sup>–1 NRZ PRBS signal. Then, the composite optical signal was launched into a 5 km long DCF followed by a 40 km long standard SMF (equivalent to the SMF-28 fiber). The DCF fiber was used to increase the Raman amplifier gain and to fully compensate for group velocity dispersion as well. Table 1 shows the attenuation and dispersion of the fibers used in our experiments. Two different sets of pump lasers were considered in the experimental evaluation. The first one had four semiconductor diode lasers with wavelengths of 1426 nm, 1444 nm, 1462 nm, and 1487 nm and pump power lower than 400 mW each. The other set used was a single high pump power laser (up to 2.0 W), whose wavelength was centered at 1480 nm.

Because of the modulator high insertion loss, an EDFA was used at the modulator output to enable signal propagation through the fiber link. The DFB lasers were set to present an output power of 0 dBm after the EDFA. Optical circulator and isolator were used to eliminate undesired back reflections. Polarization controllers were used at the modulator input and output due to its polarization dependence. The variable optical attenuator enabled signal power level variation at the EDFA input. The signal and pump waves counter-propagate inside the optical fibers. The counter-propagating configuration is preferred for system applications as pump fluctuations are averaged out [2]. The amplifier module was used to pump both SMF and DCF. The OSA resolution was equal to 0.07 nm.

Using the setup presented in Figure 1, it was possible to obtain the eye diagram, the signal-to-noise ratio (SNR), extinction ratio, optical spectrum, and power level of the four signal channels.

### 3. EXPERIMENTAL RESULTS

The continuous wave characterization of the Raman amplifier module regarding on–off gain and optical SNR was performed

considering the pump configuration shown in Figure 1. The obtained results are similar to that reported in Ref. 9 although the pump wavelengths were slightly different. In that case, the optical power of three pump lasers with wavelengths at 1453 nm, 1470 nm, and 1490 nm was coupled into the fiber end with a total pump power of 0.47 W. A gain ripple close to 6.5 dB was observed for the whole wavelength range of 100 nm. The use of optimized pump wavelengths, not available in those analyses, would minimize this high ripple observed.

#### 3.1. Multiple Pump Lasers Raman Amplifier Setting

The results obtained in the system characterization considers the four WDM input channels modulated at 40 Gb/s each and four pump lasers with power levels lower than 400 mW.

After propagating the signal channels through both fibers without Raman amplification, the eye diagram for channel  $\lambda_2$  (1550.12 nm) was measured and is illustrated in Figure 2. As expected, signal attenuation is observed when the signal propagates along the fiber link. The main source of eye degradation is due to noise. The rise time lower than 12 ps indicates that dispersion effects are practically not observed. As the dispersion management is required to transmission rates equal to 40 Gb/s, the dispersion compensation using DCF is effective to this system. In this case, the extinction ratio is 4.8 dB.

When Raman amplification is considered, the optical signal power is enhanced about 34 dB due to the amplification provided by the amplifier. Figure 3 shows the eye diagram for 1550.12 nm signal channel ( $\lambda_2$ ) at the link output when Raman amplification is used. Because of optical amplification, the eye is improved when compared to the case where no amplification is used. The SNR obtained is now 19.2 dB, the extinction ratio is 10.4 dB and the jitter is 1097 fs. Despite eye opening, noise is still a SNR degradation factor.

#### 3.2. Single High Pump Power Laser Raman Amplifier Setting

The system is now characterized using a single high pump power laser (1.0–2.0 W) as the Raman pump set.

In Figure 4, the optical spectra for one signal channel modulated at 40 Gb/s after propagating the SMF and DCF fibers are exhibited for three different pump power levels: 1.0 W, 1.5 W, and 2.0 W. Signal wavelength under observation is again  $\lambda_2$  – 1550.12 nm.

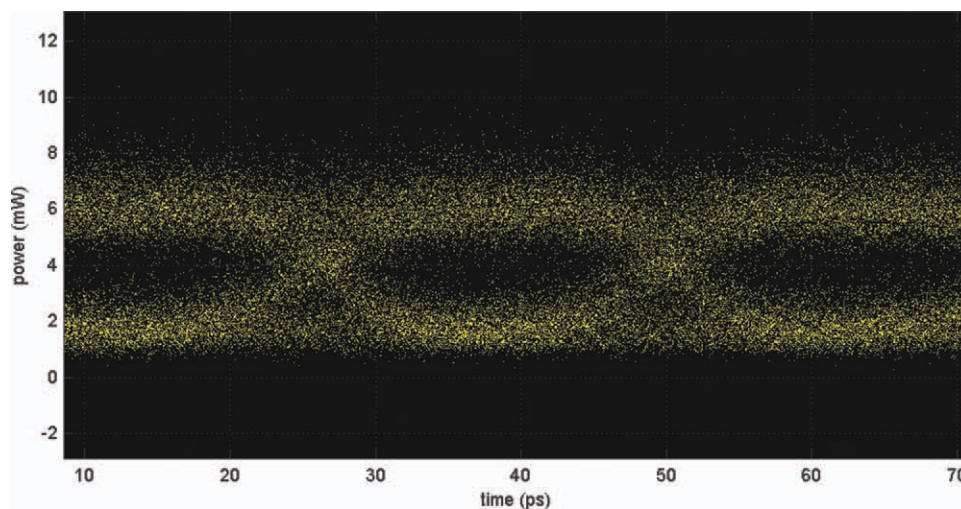


**Figure 2**  $\lambda_2$  signal channel eye diagram after propagating the SMF and DCF fibers without Raman amplification. [Color figure can be viewed in the online issue, which is available at [wileyonlinelibrary.com](http://wileyonlinelibrary.com)]

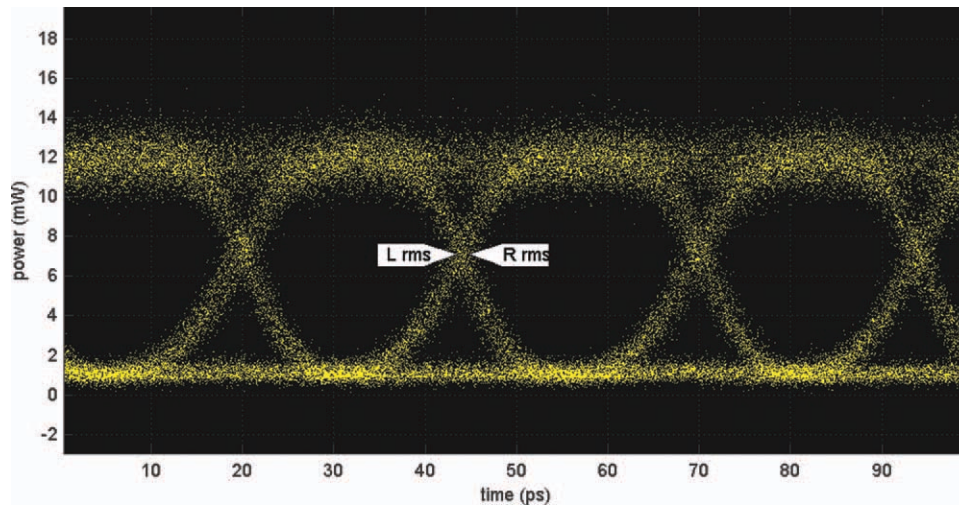


**Figure 3**  $\lambda_2$  signal channel eye diagram after propagating the SMF and DCF fibers with Raman amplification. [Color figure can be viewed in the online issue, which is available at [wileyonlinelibrary.com](http://wileyonlinelibrary.com)]

It can be seen that even for a pump power of 1 W, the Brillouin peaks are present due to the high pump power injected into the link, exhibiting, as expected an 11 GHz shift to the longer wavelength side of signal channel  $\lambda_2$ . A 10-dB signal gain is observed for a pump power of 2 W, in Figure 4. Rayleigh scattering and also double Rayleigh scattering waves are present as noted in the noise floor with an upshift of around 15 dB from the curves for 1.0–2.0 W.

When the Raman gain is very high, that is, extremely high pump power is incident into the optical fiber, Rayleigh scattering and also double Rayleigh scattering waves are generated by the pump wave and a distributed mirror is created inside the fiber.

Moreover, the interaction between the pump and the signal (Stokes field) waves also occurs through an acoustic wave. The acoustic wave modulates the refractive index of the medium creating a grating on it. This, in turn, scatters the pump light through Bragg diffraction [10]. The distributed mirror combined with the grating obtained by the acoustic wave forms a linear cavity where the Brillouin Stokes lines are generated and

assisted by Rayleigh scattering [10]. This is a possible justification explaining the Brillouin peaks in our experimental results. A further increase in pump power leads to the generation of higher order Brillouin peaks which degrade the system.

In Figure 5, the Brillouin peaks are analyzed as a function of the amplifier saturation again for the propagation of signal channel 2, merely. Considering the case of  $P_p = 1.5$  W, by increasing the signal input power from 0 to 4 dBm, no change in the output power was observed. This is an indication that the Raman amplifier is reaching saturation (indistinguishable star and triangle curves). Furthermore, the increase in pump power to 2.0 W shows a 4.2 dB of output signal power enhancement only.

To evaluate the influence of the pump power on the Brillouin effect over the four signal channels, the other channels ( $\lambda_1$ ,  $\lambda_3$ , and  $\lambda_4$ ) were added to the  $\lambda_2$  signal channel in the link. The obtained result is shown in Figure 6 for a link with SMF, DCF, and Raman amplification. The Brillouin threshold is dependent on signal energy distribution [7]. The  $\lambda_3$  and  $\lambda_4$  signal channels present first-order Brillouin lines, which are not visible in the first channel. Conversely, the  $\lambda_2$  signal channel shows higher order Brillouin lines. It was observed that there is an odd

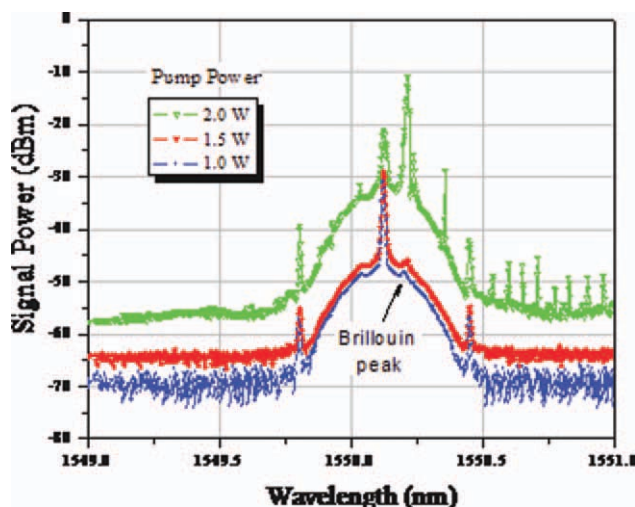


**Figure 4** Optical spectra for 40 Gb/s signal channel 2 at the link output. [Color figure can be viewed in the online issue, which is available at [wileyonlinelibrary.com](http://wileyonlinelibrary.com)]

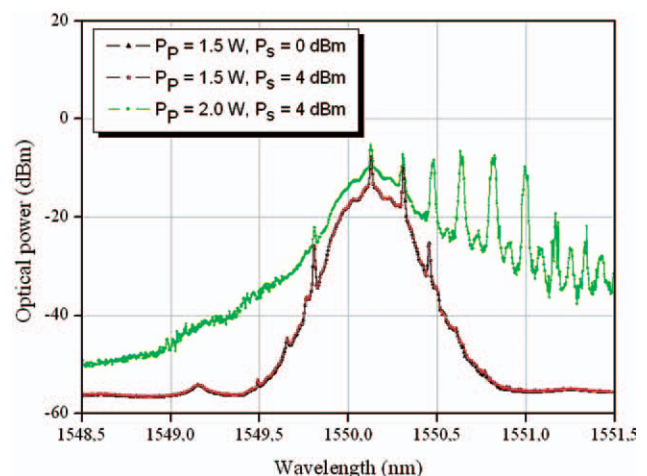


**Figure 5** Modulated signal channel 2 output spectra turned on with 0 and 4 dBm, for pump power of 1.5 and 2.0 W. [Color figure can be viewed in the online issue, which is available at [wileyonlinelibrary.com](http://wileyonlinelibrary.com)]

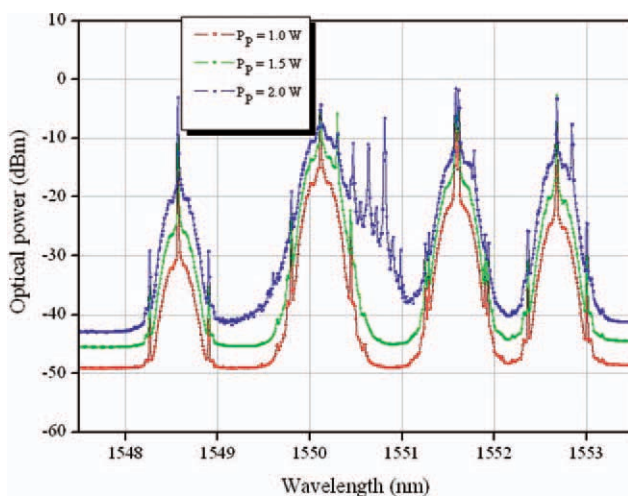
distribution of power among the channels (more than 10 dB above the other ones) even though the input signal powers presented the same values for the four signal channels. It seems that the higher sensitivity of channel 2, presented in Figure 6, is a consequence of the co-operative Raman-Rayleigh-Brillouin effect mentioned before. Comparing our quantitative results for SBS threshold power with 364 mW of total pump power, we obtained a 50-dB excursion for an input signal power varying from 0 to 10 dBm. The behavior observed in our measured results is in the same order of magnitude from the reported in Ref. 11. In that case, the SBS threshold is estimated as—4 dBm when 400 mW is used as the total counter-propagating pump power.

Figure 7 exhibits the details of the optical spectra of  $\lambda_2$  signal channel and part of the spectra of  $\lambda_1$  and  $\lambda_3$  signal channels. As can be noted, the Brillouin peaks appear to the longer wavelength side of channel  $\lambda_2$  and are extremely dependent on pump power. A pump power of 1 W is sufficient to induce Brillouin effect in channel 2. However, higher order Brillouin lines are visible for a pump power from 1.5 W onward.

Notice that the Brillouin peaks around signal channel 2 are observed despite the adjacent channels are present or not (Fig. 5). It indicates that the pump power and wavelength intensify the Brillouin effect at this specific wavelength generating higher order Brillouin lines when compared to the others signal channels. Energy interplay between channels does not seem to be relevant in the higher order Brillouin lines formation, as the peaks are observed even when only one channel is on (Fig. 5).

#### 4. CONCLUSIONS

We have analyzed experimentally a high capacity optical system with distributed Raman amplifier operating under large pump power input conditions. Raman amplification proved to enhance the channels eye diagram. Two different pump settings were considered in the study. A 5 km DCF fiber and Raman amplification guarantee a SNR of 19.2 dB, an extinction ratio of 10.4 dB and a jitter of 1097 fs for the multiple pump configuration. In the single high pump power configuration, despite the 10 dB Raman gain, power levels more than 0.5 W lead to the appearance of SBS lines which are the main contribution for system degradation.



**Figure 6** Four WDM amplified and modulated output signals. [Color figure can be viewed in the online issue, which is available at [wileyonlinelibrary.com](http://wileyonlinelibrary.com)]

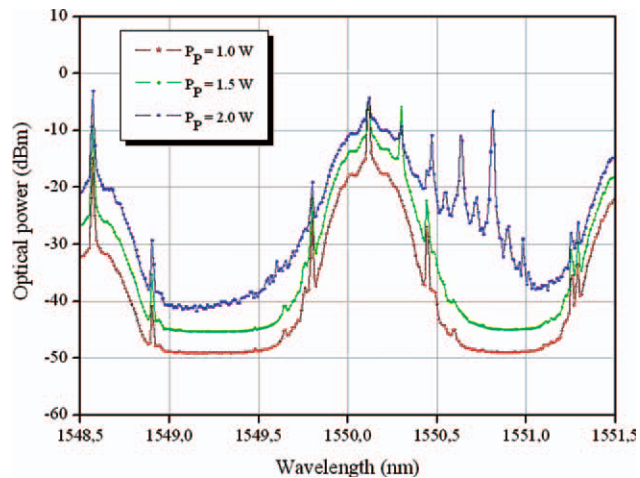


**Figure 7** Details of the modulated signal channel 2 spectra. [Color figure can be viewed in the online issue, which is available at [wileyonlinelibrary.com](http://wileyonlinelibrary.com)]

#### ACKNOWLEDGMENTS

This work was supported in part by CNPq and GRICES under Grants 490695/2006-0 and 305024/2009-4. The authors greatly acknowledge the financial support provided by FCT through FEFOF (PTDC/EEA-TEL/72025/2006) and TECLAR (POCI/A072/2005) projects.

#### REFERENCES

1. J. Wang, Y.g. Jin, C. Shen, Z. Zhang, and Y. Qiu, Gain property of Brillouin scattering in S band Raman amplifier, 2010 Symposium on Photonics and Optoelectronic, June 2010.
2. M.N. Islam, Raman Amplifiers for Telecommunications 2: Sub-Systems and Systems, Springer series in optical sciences, Berlin, Germany, 2004.
3. T. Matsuda, T. Kotanigawa, A. Naka, and T. Imai,  $62 \times 42.1$  Gbit/s (2.5 Tbit/s) WDM signal transmission over 2200 km with broadband distributed Raman amplification, Electron Lett 38 (2002), 818–819.
4. Z. Li, A. Nirmalathas, M. Bakaul, Y.J. Wen, L. Cheng, J. Chen, C. Lu and S. Aditya, Performance of WDM fiber-radio network using distributed Raman amplifier, IEEE Photon Technol Lett 18 (2006), 553–555.
5. D. Cotter, Stimulated Brillouin scattering in monomode optical fiber, J Opt Commun 4 (1983), 10–19.
6. R.G. Waarts and R.P. Braun, Crosstalk due to stimulated Brillouin-scattering in monomode fiber, Electron Lett 21 (1985), 1114–1115.
7. M.I.M. Ali, A.K. Zamzuri, A. Ahmad, R. Mohamad, and M.A. Mahdi, Experimental validation of double-pass discrete Raman amplifier limitation for large signals, IEEE Photon Technol Lett 18 (2006), 493–495.
8. M.T.M. Rocco Giraldo, A.M. Rocha, B. Neto, C. Correia, M.E.V. Segatto, M.J. Pontes, A.P.L. Barbero, J.C.W. Costa, M.A.G. Martinez, O. Frazao, J.M. Baptista, H.M. Salgado, M.B. Marques, A.L.J. Teixeira, and P. S. André, Rayleigh assisted Brillouin effects in distributed Raman amplifiers under saturated conditions at 40 Gb/s, Microwave Opt Technol Lett 52 (2010), 1331–1335.
9. M.T.M. Rocco Giraldo, A.M. Rocha, B. Neto, C. Correia, M.E.V. Segatto, M.J. Pontes, A.P.L. Barbero, J.C.W. Costa, M.A.G. Martinez, O. Frazao, J.M. Baptista, H.M. Salgado, M.B. Marques, A.L.J. Teixeira, and P.S. Andre, Brillouin effects in distributed Raman amplifiers under saturated conditions, 2009 SBMO/IEEE MTT-S International Microwave and Optoelectronics Conference, November 2009.
10. G.P. Agrawal and C. Headley, Raman amplification in fiber optical communication systems, Optics and photonics, Elsevier Academic Press, 2005.

11. M. Mehendale, A. Kobaykov, M. Vasilyev, S. Tsuda, and A. F. Evans, Effect of Raman amplification on stimulated Brillouin scattering threshold in dispersion compensating fibres, *Electron Lett* 38 (2002), 268–269.

© 2012 Wiley Periodicals, Inc.

## WIDEBAND TO NARROWBAND FREQUENCY RECONFIGURATION USING PIN DIODE

Muhamad Faizal Ismail, Mohamad Kamal A. Rahim, and Huda A. Majid

Radio Communication Engineering Department (RaCED), Universiti Teknologi Malaysia (UTM), 81310 UTM JB, Johor, Malaysia; Corresponding author: mkamal@fke.utm.my

Received 25 August 2011

**ABSTRACT:** A frequency reconfigurable antenna using log-periodic technique is reported. A 13 square patches fed by inset feed line technique are connected with a single transmission line by a log-periodic array formation to form a wideband frequency from 3 to 6 GHz. By applying 13 PIN diodes at the transmission line with a quarter wavelength radial stub biasing, three different sub-band frequencies (3–4, 3.7–5, and 4.8–6 GHz) are configured by switching ON and OFF the PIN diodes. The antenna has a directive radiation pattern and gain about 6–8 dB at all sub-bands. Simulated and measured results with antenna design are presented and they show that a good agreement in term of return loss. © 2012 Wiley Periodicals, Inc. *Microwave Opt Technol Lett* 54:1407–1412, 2012; View this article online at [wileyonlinelibrary.com](http://wileyonlinelibrary.com). DOI 10.1002/mop.26826

**Key words:** log-periodic antenna; reconfigurable frequency; PIN diode; wideband; microstrip

### 1. INTRODUCTION

In the past few decades, technology in microstrip antennas has advanced tremendously, especially in those incorporating active

components. There has been a dramatic increase in the awareness of reconfigurable antenna for applications in future wireless communications—such as cognitive radio [1], ground-penetrating radar applications [2], and RFID applications [3]. Compared with passive antennas, reconfigurable antennas provide the capability to dynamically adjust various antenna parameters—such as operating frequency [4], polarization [5], radiation pattern [6], and/or two or more of parameters [7] in a single antenna.

The advantage of frequency-reconfigurable antenna is that it can be reconfigured into any frequency in wideband range and can change dynamically, either transmitting or receiving on a single antenna instead of using multiple antennas as usual. For radar application or smart weapon detection, it is advantageous to vary the beam shaping functionality in that system. Besides that, the reconfigurable antenna can also reduce any unfavorable effects from congested signals especially in Instruments, Scientific and Measurement (ISM) band (2.4 and 5.8 GHz) and also caused by cosite interference and jamming effect.

The monopole wideband antenna is also proposed for reconfigurable purposes [8] because of various advantages: low profile, thin and small, ability to produce very wide frequencies, and possession of an omnidirectional pattern. The cognitive communication system requires wideband antennas for spectrum sensing and narrow band antennas for transmission, which has a directional radiation pattern to increase the performance of signal detection. The development of wideband reconfigurable antenna with directional radiation pattern has been reported in Ref. 9. The antenna should be well suited in cost, radiation pattern, gain, and ease of integration with switching circuitry.

In this article, a reconfigurable log-periodic antenna (RLPA) is developed to meet these requirements. The log-periodic technique is used in microstrip array formation to obtain wideband operating frequency. The PIN diode switches are incorporated with the line feed of each patch to provide reconfigurability operation. This antenna is fed by a normal inset feed with transmission lines compared with Ref. 1, where aperture couple slot-fed was used. This technique may produce an error in misalignment of patch with slot, and it can reduce the performance

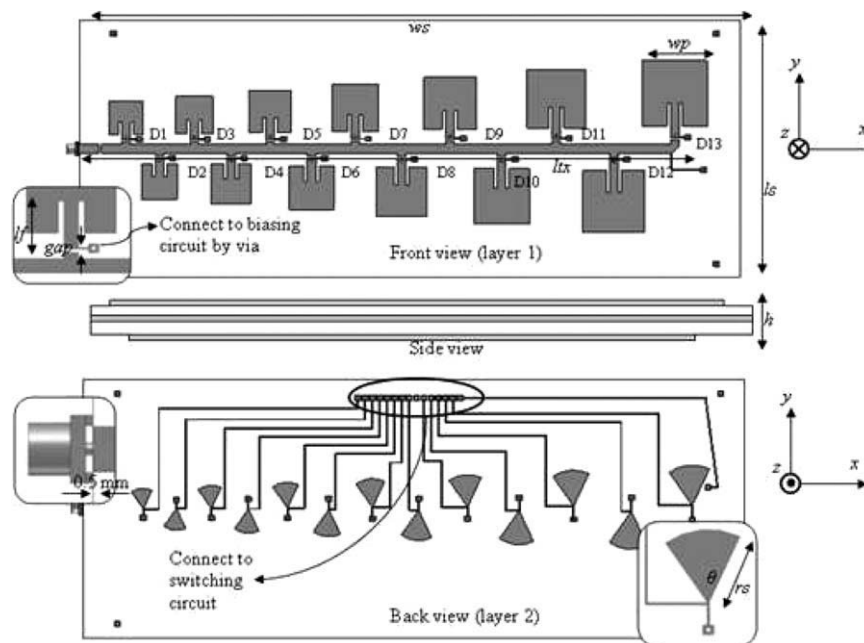


Figure 1 The configuration of frequency RLPA